Supplementary Materials

Supplementaary Fig. 1

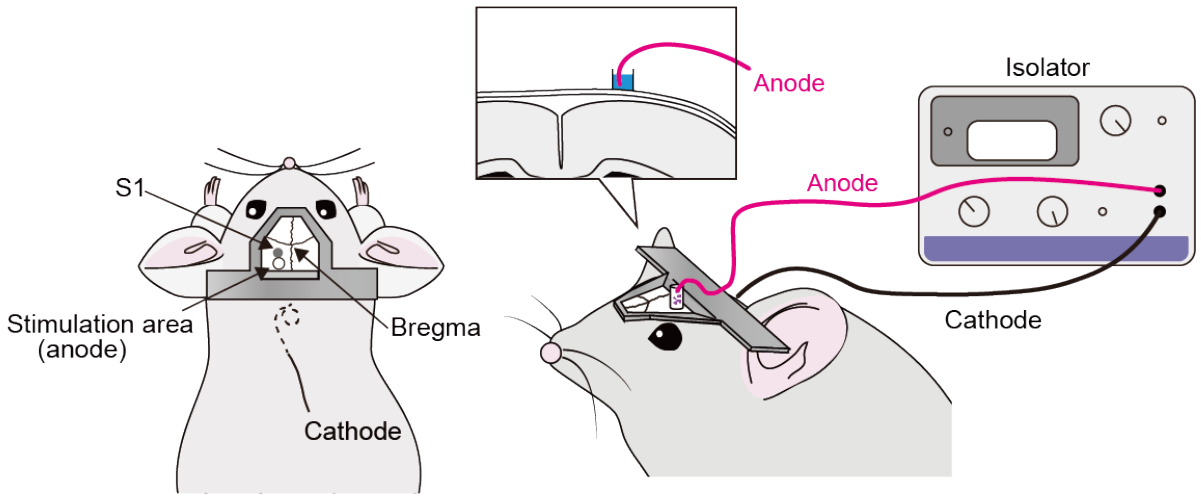

Supplementary Fig. 1. Schematic of the tDCS setup.

During tDCS, direct current was applied from the anode to the cathode using a stimulus isolator. The anode site consisted of an area of exposed skull that was located 2 mm posterior to the left S1, i.e., the side contralateral to the PSL injury. The anode site was covered with conductive gel into which was placed a silver wire. The cathode consisted of a silver wire that was sutured under the skin at the neck.

Supplementary Fig. 2

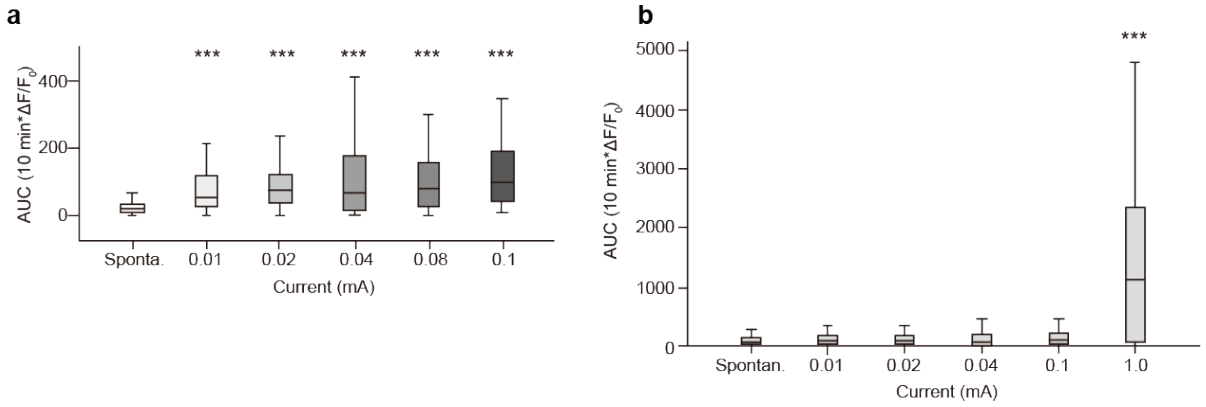

Supplementary Fig. 2. Astrocytic and Neuronal Ca^{2+} responses at different tDCS current intensities.

a Astrocytic Ca^{2+} responses (n = 66 astrocytes from 3 mice) were recorded in awake mice during tDCS sessions in which the amplitude of the steady current applied over a 10-minute session varied from between 0.01 mA and 0.1 mA. The integral of Ca^{2+} events over the 10 mins was summed. Differences between spontaneous Ca^{2+} activity levels (Spontan.) and those at each of the different tDCS current intensities was compared using one-way repeated measures ANOVA, $F(1.442, 315) = 58.078$, $p = 0.000$; followed by a Bonferroni post-hoc test, vs 0.01 mA (p = 0.000), vs 0.02 mA ($p = 0.000$), vs 0.04 mA ($p = 0.000$), vs 0.08 mA ($p = 0.000$), vs 0.1 mA (p = 0.000), *** $p < 0.001$. Based on this data, tDCS using a constant current of 0.01 mA for 10 minutes was used to induce elevated astrocyte Ca^{2+} activity in subsequent experiments.

b Neuronal Ca^{2+} responses (n = 180 neurons from 4 mice) were recorded in awake mice during tDCS sessions in which the amplitude of the steady current applied over a 10-minute session varied from between 0.01 mA and 0.1 mA. The integral of Ca^{2+} events over the 10 mins was summed. Differences between spontaneous Ca^{2+} activity levels (Spontan.) and those at each of the different tDCS current intensities was compared using one-way repeated measures ANOVA, $F(1.331, 895) = 166.858$, $p = 0.000$; followed by a Dunnett post hoc test, vs 0.01 mA ($p = 1.000$), vs 0.02 mA ($p = 1.000$), vs 0.04 mA ($p = 1.000$), vs 0.1 mA ($p = 0.214$), vs 1.0 mA ($p = 0.000$), *** $p < 0.001$. Elevated neuronal Ca^{2+} responses were not induced at tDCS current intensities less than 1.0 mA. These experiments confirmed the astrocyte specificity of 0.1 mA current intensity tDCS.

Supplementary Fig. 3

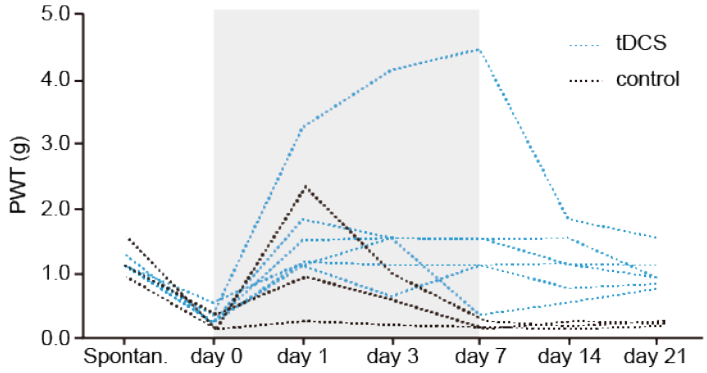

Supplementary Fig. 3. Mechanical thresholds in individual mice with tDCS application.

Blue dotted-lines show the withdrawal thresholds in each mouse with the combined tDCS-TTX treatment, while black dotted-lines show the data for each control-TTX mouse. The period of tDCS-TTX therapy is indicated by the grey shading. Group data is shown in the main text Fig. 1d.

Supplementary Fig. 4

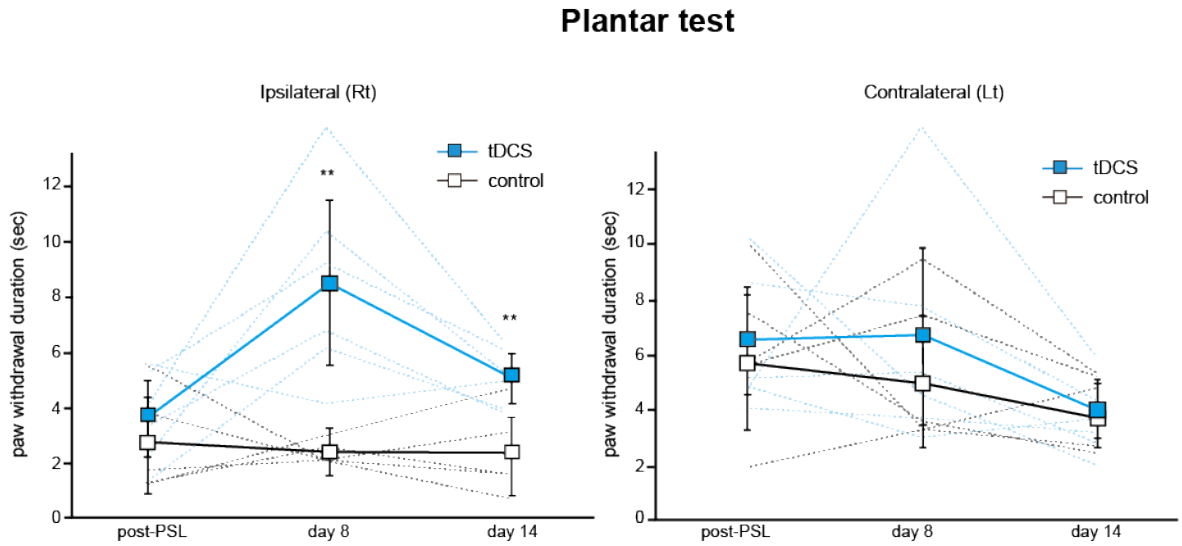

Supplementary Fig. 4. tDCS also reverses thermal allodynia

The plantar test, which measured paw withdrawal time following application of an infrared heating beam, was used to assess thermal pain sensation. Left graph shows the withdrawal latencies of the injured right hind paw, while the left panel shows the withdrawal latencies of the intact, contralateral, left hind paw. Withdrawal latencies were assessed post-PSL and post treatment (day 8 and 14), for control and for tDCS/TTX treatment groups. After treatment, withdrawal latencies in the tDCS-treated group (blue line, $n = 6$, dotted lines show individual data traces) were significantly increased as compared with control group (black line, $n = 5$, dotted lines show individual data traces) for the injured paw, with no differences for the intact side. Comparisons between control and tDCS mice at each time point were tested using a two-way

repeated measures ANOVA, Injured side (right hind paw); $F(2, 18) = 5.112$, $p = 0.017$, followed by a Bonferroni post hoc test, post-PSL ($p = 0.404$), day 8 ($p = 0.004$), day 14 ($p = 0.007$). Intact side (left hind paw); interaction effect, $F(2, 18) = 0.236$, $p = 0.792$, main effect, $F(1, 9) = 0.769$, $p = 0.403$.

Supplementary Fig. 5

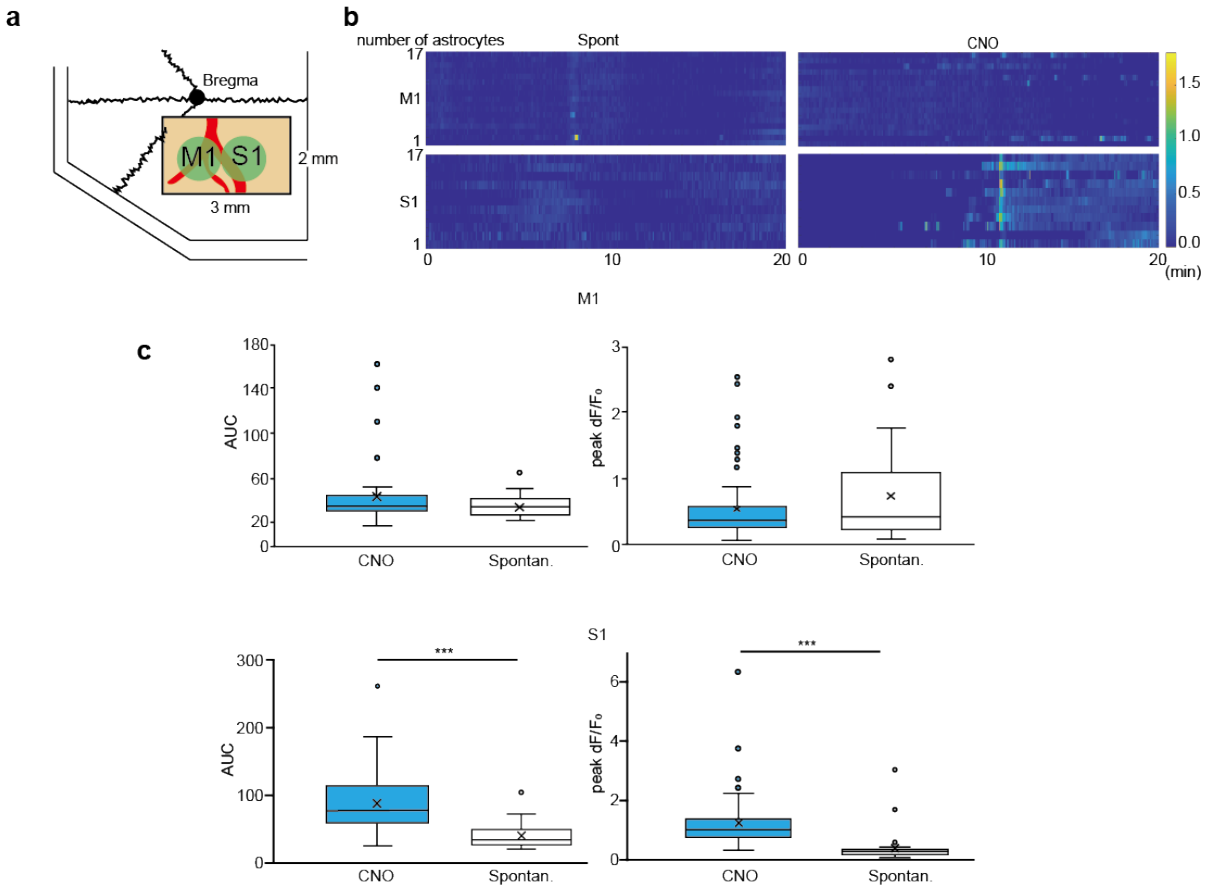

Supplementary Fig. 5. CNO injection increases the activitiy of S1 astrocytes, but not of M1 astrocytes.

a Schematic of M1 and S1 astrocyte Ca^{2+} imaging. AAV-GFAP-GCaMP6f was injected into both M1 and S1, while AAV-GFAP-hM3D-mCherry was injected just into S1.

b Representative date of M1 and S1 astrocyte Ca^{2+} imaging from a mouse. A single injection of CNO induces an increase in S1 astrocytic Ca^{2+} activity, but dos not change M1 astrocytic Ca^{2+} activity. Left panels show baseline Ca^{2+} activity, right panel show activity after a single CNO injection for 17 different

M1 (upper) and S1 (lower) astrocytes. M1 and S1 imaging was performed on different days with 17 astrocytes in one plane imaged each time in either S1 or M1, but with all imaging done in the same mice and with at least 3 days between the 1st and second CNO injections.

c Mean integrals and peak amplitudes of the Ca^{2+} responses from M1 astrocytes (upper, $n = 51$ astrocytes from 3 mice) and S1 astrocytes (lower, $n = 33$ astrocytes from 3 mice). Comparions between spontaneous Ca^{2+} transients and (in the same cell) after a single injection of CNO used paired samples *t* test: AUC, M1; $p = 0.061$, S1; $p = 0.000$, peak dF/F0, M1; $p = 0.107$, S1; $p = 0.000$).

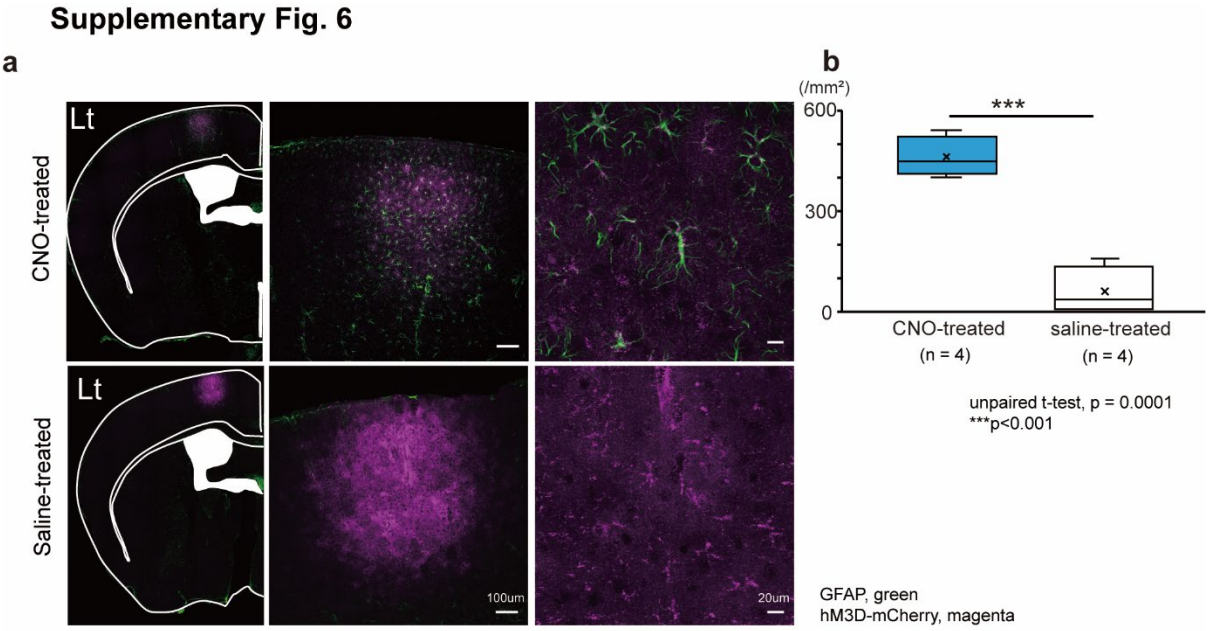

Supplementary Fig. 6. Repeated activation of S1 astrocytes induces GFAP expression.

After multiple (12) CNO injections, intense GFAP staining was observed in S1, indicating astrocyte activation.

a Immunohistochemistry showing localized expression of GFAP (green) and mCherry-hM3D (magenta) in S1 cortex (left panel). Middle and right panels show higher magnification (scale bar = 100 μm middle; 20 μm right).

b Box plot show the density of GFAP-positive cells from CNO-treated ($n = 4$) and saline-treated ($n = 4$) mice. GFAP expression increased in CNO-treated mice as compared with saline-treated mice. unpaired t test, p = 0.0001.

Supplementary Fig. 7

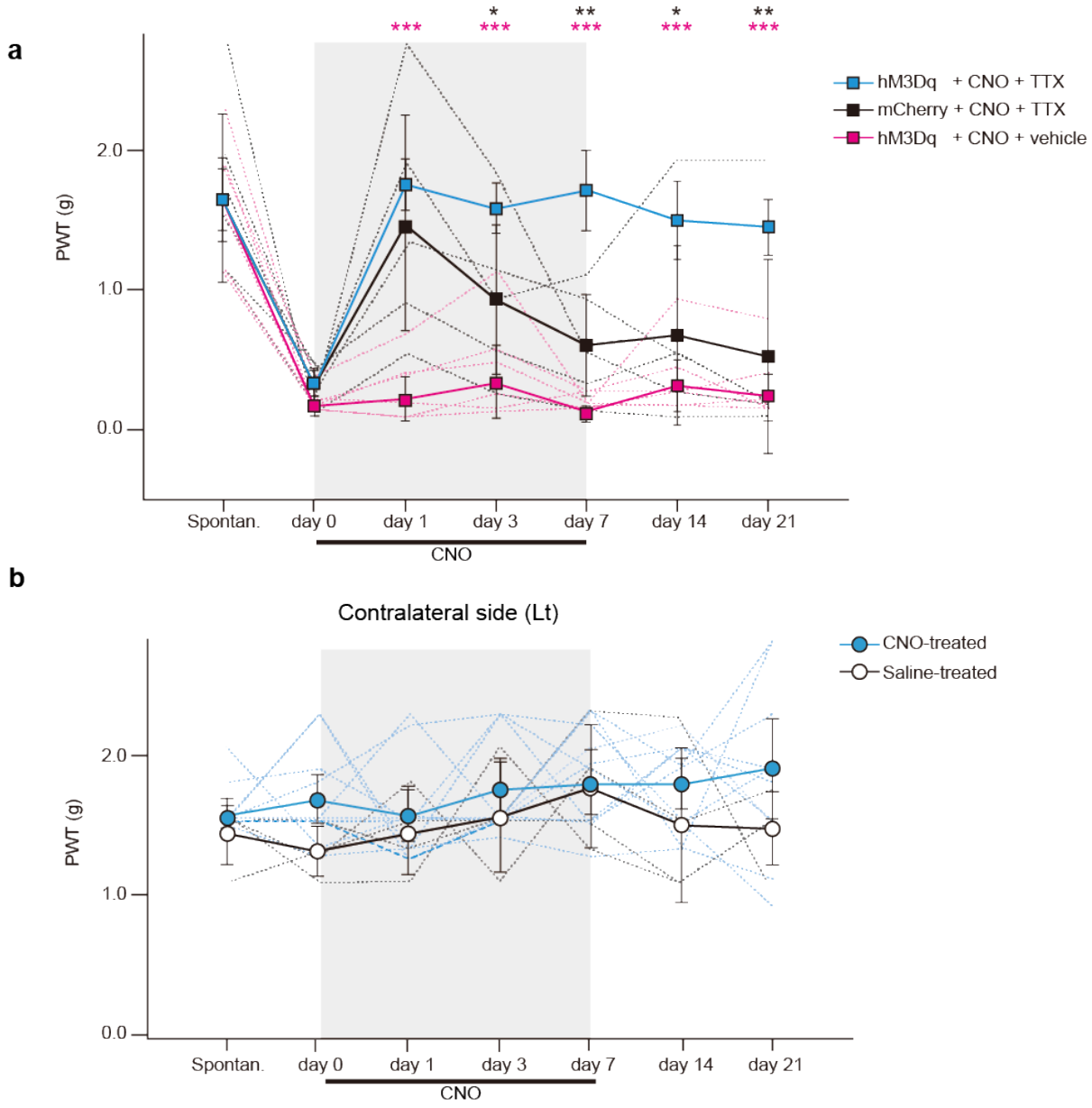

Supplementary Fig. 7. CNO (1.0 mg/kg) treatment only reverses allodynia in mice expressing hM3D in astrocytes and with concurrent TTX application.

a Control experiments to accompany Fig. 2d in the main text showing paw withdrawal thresholds in different mice cohorts. The graph showing the effects of combined CNO-TTX treatment to

reverse mechanical allodynia induced by prior PSL injury in mice expressing hM3D in astrocytes (blue squares, n = 13 mice) was reported in Fig. 2d and shown again here alongside a number of controls where mechanical thresholds remained hypersensitive: PSL mice with CNO-induced astrocyte activation but without TTX-blockade of peripheral afferents (hM3D-CNO-vehicle mice; magenta line, n = 8); PSL mice with mCherry expression only, but treated with CNO and TTX (note the transient reversal of allodynia due to TTX; black line, n = 5). Comparisons between hM3D-CNO-TTX mice and either the hM3D-CNO-vehicle mice or the mCherry-CNO-TTX mice at each time point before, during and after treatment was tested using a two-way repeated measures ANOVA, $F(7.323, 84.209) = 8.937$, $p = 0.000$, followed by a Bonferroni post hoc test, Spontan. ($p = 1.000$ and $p = 1.000$), day 0 ($p = 0.039$ and $p = 1.000$), day 1 ($p = 0.000$ and $p = 0.819$), day 3 ($p = 0.000$ and $p = 0.014$), day 7 ($p = 0.000$ and $p = 0.000$), day 14 ($p = 0.000$ and $p = 0.012$), and day 21 ($p = 0.000$ and $p = 0.001$) with the first and second p-value per set referring to hM3D-CNO-TTX vs hM3D-CNO-vehicle and hM3D-CNO-TTX vs mCherry-CNO-TTX respectively. These results confirm chronic pain is cured only through simultaneous

astrocyte activation with peripheral afferent blockade, without contributions from potential non-astrocyte related effects of CNO.

b Mechanical thresholds from the contralateral, uninjured paw are unaffected by CNO (1.0 mg/kg) treatment. Mechanical thresholds for paw withdrawal following von Frey hair stimulation of the contralateral (left) uninjured paw remained unchanged as compared to the control levels (Spontan.), i.e., before PSL in the right paw, by CNO-TTX or saline-TTX treatment. Comparisons between CNO- (n = 11) and saline-treated mice (n = 5) at each time point was tested using a two-way repeated measures ANOVA, $F(6, 78) = 0.484$, $p = 0.819$, followed by a Bonferroni post hoc tests, 1.0 mg/kg CNO-treated (n = 11 mice) vs saline-treated mice (n = 5 mice), Spontan. ($p = 0.126$), day 0 ($p = 0.063$), day 1 ($p = 0.519$), day 3 ($p = 0.437$), day 7 ($p = 0.908$), day 14 ($p = 0.260$), and day 21 ($p = 0.176$). These results confirm that CNO itself has no effect on tactile and nociceptive perception processing independent of hM3D expression in S1 astrocytes.

Supplementary Fig. 8

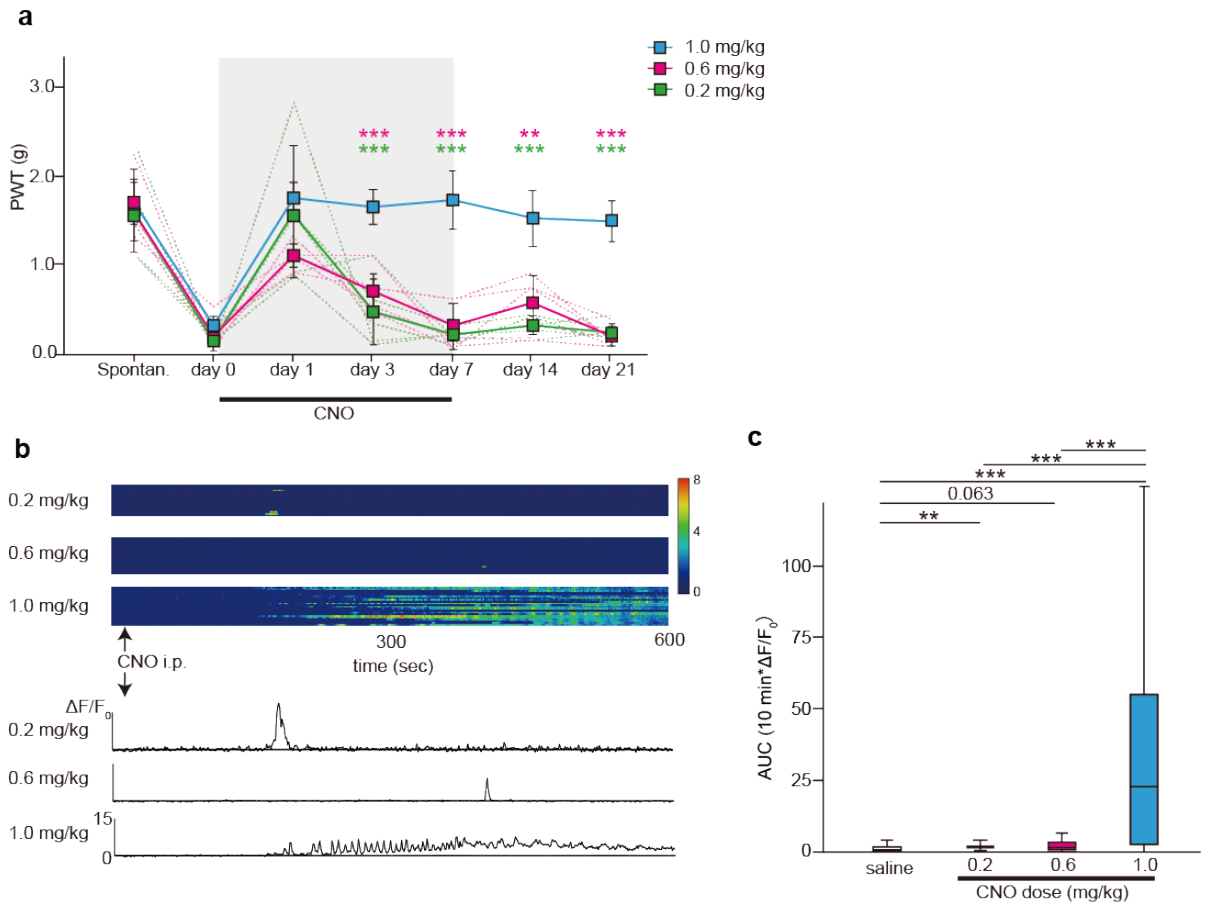

Supplementary Fig. 8. Optimizing the CNO dose to reverse allodynia.

Repeating the 1.0 mg/kg CNO-TTX treatment regimen with lower doses of CNO (0.2 or 0.6 mg/kg) failed to achieve long term reversal of allodynia (**a**), and lower CNO doses causes much smaller increases in astrocytic Ca^{2+} activity (**b** and **c**).

a Different CNO doses (0.2, 0.6, 1.0 mg/kg) were trialled using the same CNO-TTX treatment regimen. Comparisons between 1.0 mg/kg (n = 12 mice) and either 0.6 mg/kg (n = 5 mice) or 0.2 mg/kg (n = 5 mice) at each time point was tested using a two-way repeated measures ANOVA,

F(8.44, 80.216) = 6.523, $p = 0.000$; followed by Bonferroni post hoc tests, Spontan. ($p = 1.000$ and $p = 1.000$), day 0 ($p = 0.239$ and $p = 0.778$), day 1 ($p = 1.000$ and $p = 0.059$), day 3 ($p = 0.000$ and $p = 0.000$), day 7 ($p = 0.000$ and $p = 0.000$), day 14 ($p = 0.000$ and $p = 0.002$), and day 21 ($p = 0.000$ and $p = 0.000$), with the first and second p-value per set referring to 1.0 mg/kg vs 0.6 mg/kg and 1.0 mg/kg vs 0.2 mg/kg respectively.

b In the upper panel, sample raster plots show the change in fluorescence indicative of Ca^{2+} activity over 10 minutes from individual S1 astrocytes from a mouse injected with doses of CNO (0.2 mg/kg, 0.6 mg/kg, and 1.0 mg/kg). In the lower panels, traces plot the change in Ca^{2+} activity for a representative S1 astrocyte following different doses of CNO (0.2 mg/kg, 0.6 mg/kg, and 1.0 mg/kg). Arrows indicate time at which CNO was administered through intraperitoneal injection. Ca^{2+} imaging was conducted using 2-photon microscopy with mice anaesthetized with 1% isoflurane and secured via a head plate into a custom designed frame.

c Integrals of Ca^{2+} transients in individual astrocytes (ROIs traced around the soma) during 10 minutes following saline ($n = 88$ astrocytes from 3 mice) or CNO (0.2 mg/kg, $n = 52$ astrocytes from 3 mice; 0.6 mg/kg, $n = 48$ astrocytes from 3 mice; 1.0 mg/kg, $n = 76$ astrocytes from 3

mice) injections were summed for each treatment cohort. The level of Ca^{2+} activity in 1.0 mg/kg CNO-treated mice was significantly higher as compared with all other treatment cohorts. There was no significant difference in the level of Ca^{2+} activity following administration of lower CNO doses or saline. Statistical significance was tested using a Kruskal-Wallis H test, $p = 0.000$, followed by Bonferroni post-hoc test, saline vs 0.2 mg/kg ($p = 0.001$), saline vs 0.6 mg/kg ($p = 0.063$), saline vs 1.0 mg/kg ($p = 0.000$), 0.2 mg/kg vs 1.0 mg/kg ($p = 0.000$), and 0.6 mg/kg vs 1.0 mg/kg ($p = 0.000$). $^{**}p < 0.01$. $^{***}p < 0.0001$.

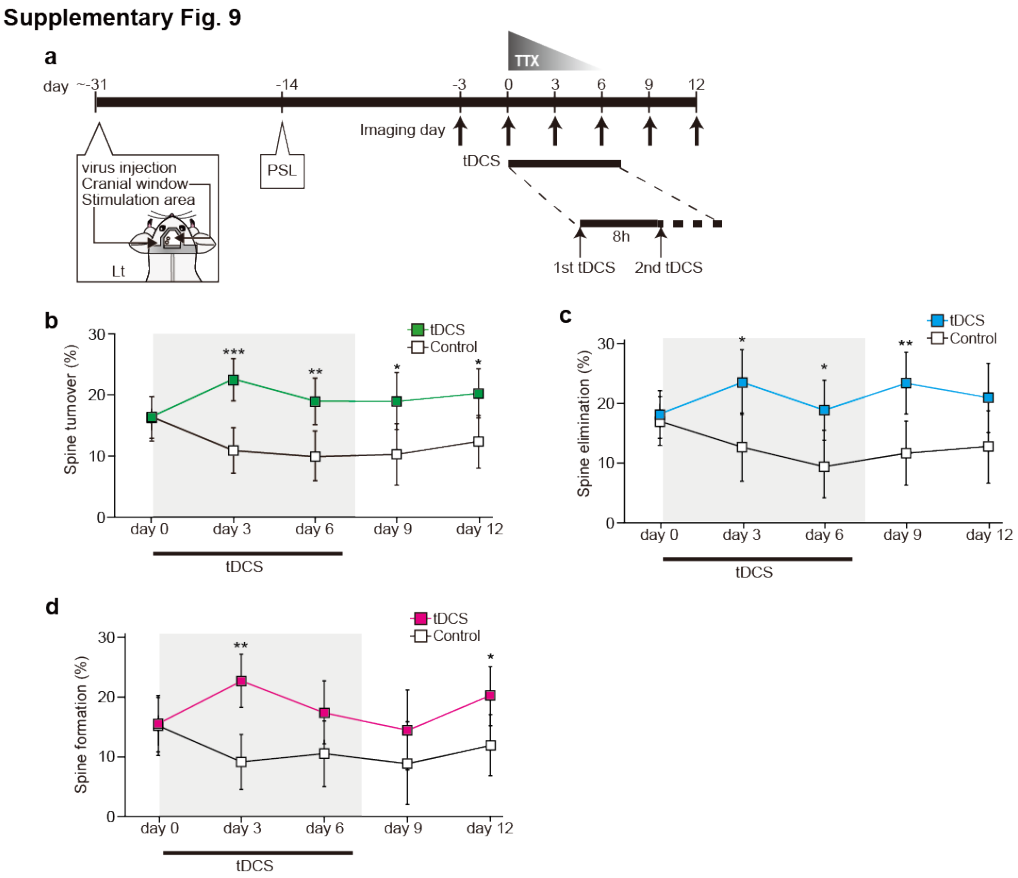

Supplementary Fig. 9. An increase in dendritic spine turnover is correlated with the reversal of mechanical allodynia.

a Schematic experimental timeline for combined neuronal imaging and treatment of PSL-induced mechanical allodynia using tDCS / TTX therapy. Spine dynamics were observed by repeated imaging of the same layer 5 pyramidal neurons in the left S1 every three days using in vivo 2-photon imaging at times indicated by the dark arrows before (day -3, 0), during (days 3 and 6) and after (days 9 and 12) tDCS treatment.

(**b** to **d**) Spine dynamics during and after tDCS (with TTX) treatment. The period during treatment is indicated by grey shading. Spine counts used for the calculations within each treatment cohort are as follows: control mice (n = 14 dendrites, 4 mice), tDCS mice (n = 16 dendrites from 3 mice), *p < 0.05, **p < 0.01, ***p < 0.001. **b** Comparisons between spine turnover rates in tDCS mice (green) and control mice (white) on each observation day used a two-way repeated ANOVA, the interaction effect: F(2.904, 81.318) = 3.718, p = 0.016; followed by Bonferroni post hoc test, day 0 (p = 0.941), day 3 (p = 0.000), day 6 (p = 0.004), day 9 (p = 0.017), and day 12 (p = 0.012). **c** Comparisons between spine elimination rates in tDCS mice (blue) and control mice (white) on each observation day used a two-way repeated ANOVA, the interaction effect: F(4, 112) = 1.717, p = 0.160, the main effect of group: F(1, 28) = 14.972, p = 0.001; followed by a Bonferroni post-hoc test, day 0 (p = 0.805), day 4 (p = 0.011), day 7 (p = 0.008), day 11 (p = 0.005), and day 14 (p = 0.060). **d** Comparisons between spine formation rates in tDCS mice (magenta) and control mice (white) on each observation day used a two-way repeated ANOVA, the interaction effect: F(3.151, 88.220) = 1.824, p = 0.146, the main effect:

1 $F(1, 28) = 9.996$, $p = 0.004$; followed by Bonferroni post hoc test, day0 ($p = 0.925$), day3 ($p =$

2 0.001), day6 ($p = 0.058$), day9 ($p = 0.200$), and day12 ($p = 0.032$).

Supplementary Fig. 10

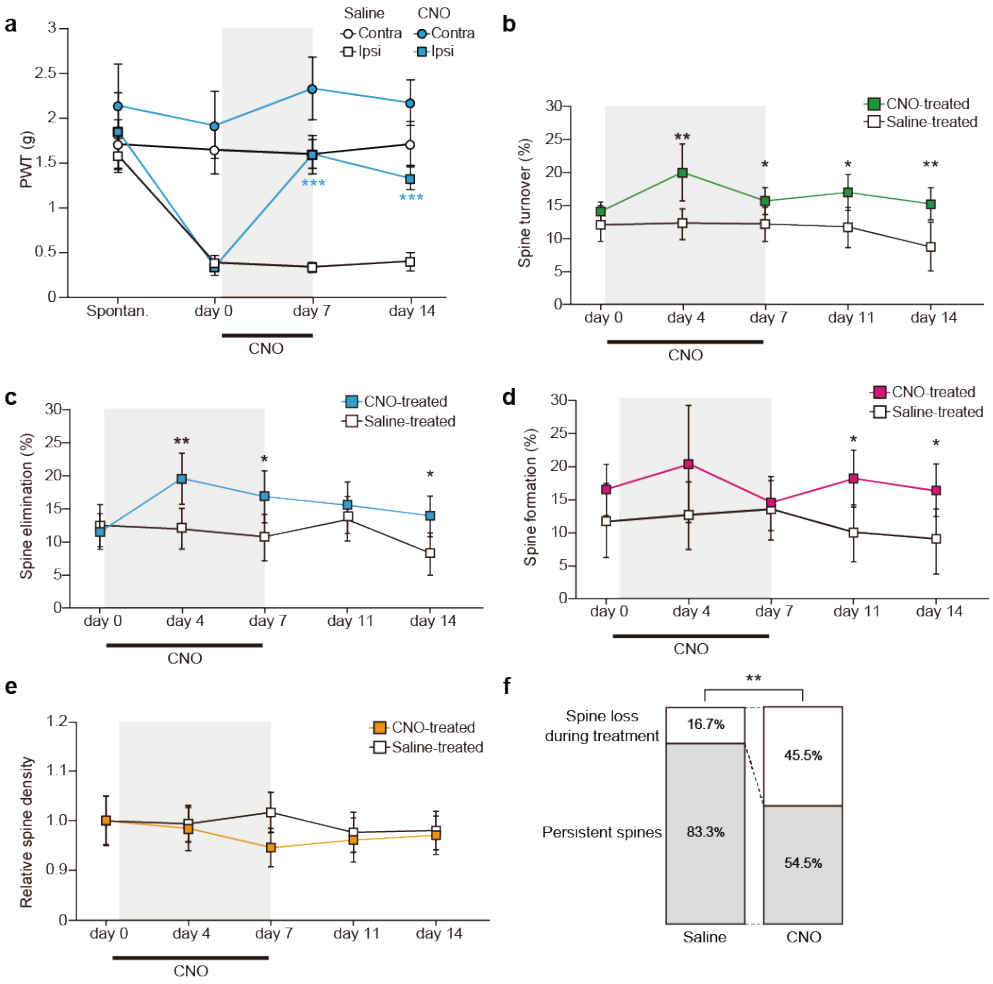

Supplementary Fig. 10. Expanded analysis on the CNO induced changes on spine dynamics. **a** The paw withdrawal thresholds in mice with prior PSL injury were also monitored throughout the long-term spine imaging and CNO-TTX treatment. The PSL operation was performed on the right sciatic nerve, TTX-Elvax cuff was plied to this injured nerve, and withdrawal thresholds examined in response to stimulation of both the injured and uninjured (left) sciatic nerve. The

period of CNO-TTX or saline-TTX treatment is indicated by grey shading. Treatment cohorts are as follows: CNO- treated mice ($n = 5$), control saline-treated mice ($n = 7$). As expected, mechanical hypersensitivity was never observed in response to stimulation of the uninjured paw for both CNO-treated and saline-treated mice. Mechanical hypersensitivity in response to stimulation of the injured paw was reversed in CNO-treated mice. Comparisons between the two paw responses and between CNO-treated and saline-treated mice at each time point used a two-way repeated measures ANOVA, $F(3,30) = 8.794$, $p < 0.001$; followed by a Bonferroni post hoc test, Spontan. ($p = 0.496$), day 0 ($p = 0.650$), day 7 ($p < 0.001$), and day 14 ($p < 0.001$). ***$p < 0.001$.

(**b** to **d**) Absolute values of relative spine dynamics, as compared to the values in Fig. 3, c to d of the main text where spine turnover, elimination and formation rates were normalized to the day 0 values. Note here, however, the variation in the day 0 values between CNO-treated and saline-treated mice. Hence plots of the non-normalized spine dynamics with their statistical analysis are also included here. The period during CNO-TTX or saline-TTX administration is indicated by grey shading. Spine counts used for the calculations within each treatment cohort are as follows: saline-treated mice ($n = 16$ dendrites, 7 mice), CNO-treated mice ($n = 19$ dendrites from 5 mice), *$p <$

0.05, **$p < 0.01$. **b** Spine turnover rate was calculated as the sum of spines that were either formed and lost between 2 successive imaging sessions, divided by the total number of spines counted in the prior imaging session. Comparisons between spine turnover rates in CNO-treated mice (green) and saline-treated mice (white) on each observation day used a two-way repeated ANOVA, the interaction effect: $F(3.050, 100.634) = 1.494$, $p = 0.22$, the main effect for group: $F(1, 33) = 19.329$, $p = 0.000$); followed by Bonferroni post hoc test, day 0 ($p = 0.276$), day 4 ($p = 0.004$), day 7 ($p = 0.045$), day 11 ($p = 0.010$), and day 14 ($p = 0.004$). **c** Spine elimination rate was calculated as the number of spines that were lost between 2 successive imaging sessions divided by the total number of spines counted in the prior imaging session. Comparisons between spine elimination rates in CNO-treated mice (blue) and saline-treated mice (white) on each observation day used a two-way repeated ANOVA, the interaction effect: $F(4, 132) = 1.834$, $p = 0.126$, the main effect of group: $F(1, 33) = 11.919$, $p = 0.002$; followed by a Bonferroni post-hoc test, day 0 ($p = 0.653$), day 4 ($p = 0.005$), day 7 ($p = 0.038$), day 11 ($p = 0.466$), and day 14 ($p = 0.019$). **d** Spine formation rate was calculated as the number of spines that were formed between 2 successive imaging sessions, divided by the total number of spines counted in the prior imaging session. Comparisons between

spine formation rates in CNO-treated mice (magenta) and saline-treated mice (white) on each observation day used a two-way repeated ANOVA, the interaction effect: $F(2.773, 91.504) = 0.671$, $p = 0.613$, the main effect: $F(1, 33) = 17.950$, $p = 0.000$; followed by Bonferroni post hoc test, day0 ($p = 0.102$), day4 ($p = 0.140$), day7 ($p = 0.707$), day11 ($p = 0.013$), and day14 ($p = 0.031$).

e Normalized spine density in CNO-TTX treated mice (yellow; $n = 19$ dendrites from 5 mice) and saline-TTX treated mice (white; $n = 16$ dendrites from 7 mice). Spine density was calculated by dividing the number of counted spines by the dendrite length. These values were then normalized against the day 0 spine density values. Comparisons between normalized spine densities in CNO-treated and saline-treated mice used a two-way repeated ANOVA, the interaction effect: $F(3.185, 105.100) = 0.645$, $p = 0.597$. There was no significant interaction between the treatment cohort and the observation day.

f Spines formed in the week following PSL, but before starting treatment, in saline-TTX treated mice ($n = 42$ spines, 16 dendrites, 7 mice) and CNO-TTX treated mice ($n = 55$ spines, 19 dendrites, 5 mice) were divided into 2 categories based on whether they were lost during treatment (Spine loss during treatment) or were still present at 7 days after the end of treatment, i.e., at day 14

(Persistent). The proportions of these 2 categories were significantly different between saline-treated and CNO-treated mice, $\chi^2(1) = 8.928$, $p = 0.003$, $^{**}p < 0.01$.

Supplementary Fig. 11

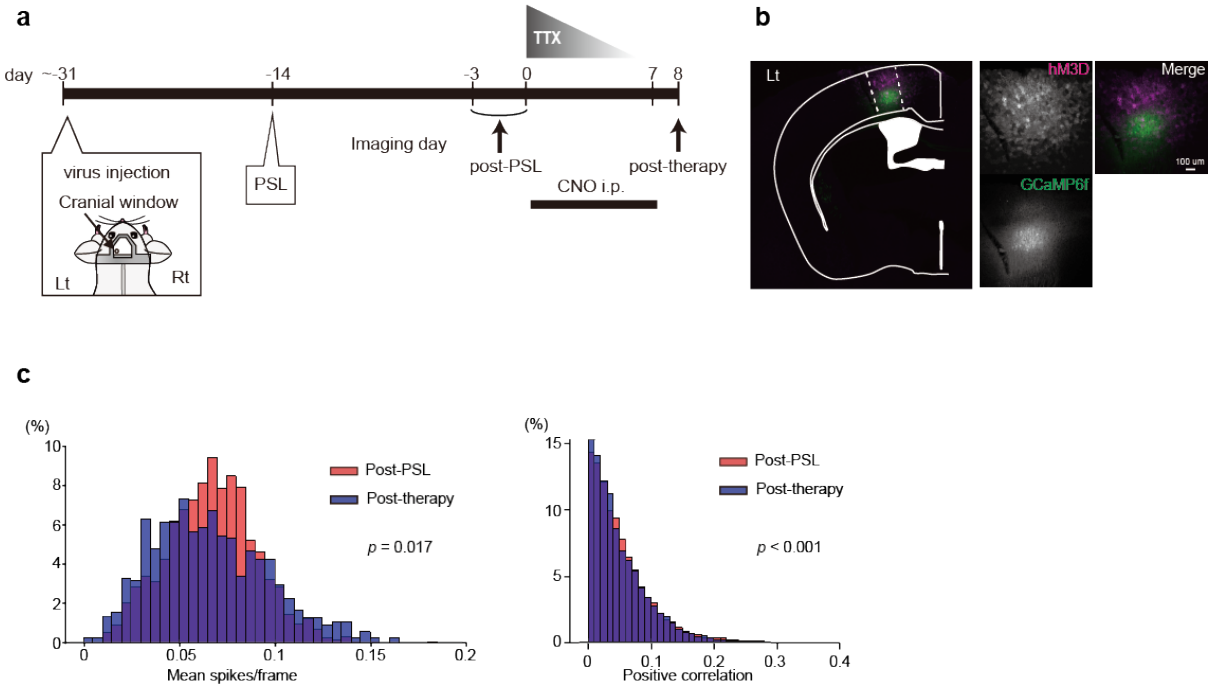

Supplementary Fig. 11. Influence to neuronal Ca^{2+} activities by therapy.

a Schematic experimental timeline for neuronal Ca^{2+} imaging before and after treating PSL-induced mechanical allodynia using the CNO-TTX therapy. Ca^{2+} imaging used in vivo 2-photon microscopy at times indicated by dark arrows.

b Sample immunohistochemistry image showing expression of hM3D-mCherry (magenta) and GCaMP6f (green) in S1 cortex. GCaMP6f was mainly expressed in layer 5 neurons and hM3D expressed in layer 3 astrocytes.

c Distribution of neuronal activity before and after CNO-TTX therapy as quantified by histograms of the mean frequency of Ca^{2+} transients in each neuron (left) and of the temporal correlation

between Ca^{2+} spikes across S1 neurons (right). Data comes from 1151neurons in 8 mice, before and 1031 neurons in 8 mice after CNO / TTX -treated mice. Both parameters decreased post-therapy (magenta) compared to post-PSL but before therapy (blue); Wilcoxon rank sum test, mean spikes ($p = 0.017$), positive correlation ($p = 0.000$).